Physiologically-relevant levels of sphingomyelin, but not GM1, induces a beta-sheet-rich structure in the amyloid-beta(1-42) monomer

Owen, Michael C.

2018-09

Owen , M C , Kulig , W , Poojari , C , Rog , T & Strodel , B 2018 , ' Physiologically-relevant levels of sphingomyelin, but not GM1, induces a beta-sheet-rich structure in the amyloid-beta(1-42) monomer ' , Biochimica et Biophysica Acta. Biomembranes , vol. 1860 , no. 9 , pp. 1709-1720 . https://doi.org/10.1016/j.bbamem.2018.03.026

http://hdl.handle.net/10138/300673
https://doi.org/10.1016/j.bbamem.2018.03.026

Physiologically-relevant levels of sphingomyelin, but not GM1, induces a β-sheet-rich structure in the amyloid-β(1-42) monomer

Michael C. Owen, Waldemar Kulig, Chetan Poojari, Tomasz Rog, Birgit Strodel

PII: S0005-2736(18)30106-8
DOI: doi:10.1016/j.bbamem.2018.03.026
Reference: BBAMEM 82751

To appear in:

Received date: 31 January 2018
Revised date: 29 March 2018
Accepted date: 31 March 2018

Please cite this article as: Michael C. Owen, Waldemar Kulig, Chetan Poojari, Tomasz Rog, Birgit Strodel , Physiologically-relevant levels of sphingomyelin, but not GM1, induces a β-sheet-rich structure in the amyloid-β(1-42) monomer. The address for the corresponding author was captured as affiliation for all authors. Please check if appropriate. Bbamem(2018), doi:10.1016/j.bbamem.2018.03.026

Physiologically-Relevant Levels of Sphingomyelin, but not GM1, Induces a β-Sheet-Rich Structure in the Amyloid-β(1-42) Monomer

Michael C. Owen,[1,2,*] Waldemar Kulig,[3] Chetan Poojari,[3,4] Tomasz Rog,[3,4] Birgit Strodel[1,5,*]

[1] Institute of Complex Systems: Structural Biochemistry (ICS-6), Forschungszentrum Jülich, 52425 Jülich, Germany
[2] CEITEC – Central European Institute of Technology, Masaryk University, Kamenice 753/5, Brno 625 00, Czech Republic
[3] Department of Physics, University of Helsinki, P.O. Box 64, FI-00014 Helsinki, Finland
[4] Department of Physics, Tampere University of Technology, P.O. Box 692, FI-33101 Tampere, Finland.
[5] Institute of Theoretical and Computational Chemistry, Heinrich Heine University Düsseldorf, Universitätsstrasse 1, 40225 Düsseldorf, Germany
* michael.owen@ceitec.muni.cz, b.strodel@fz-juelich.de

KEYWORDS: peptide-membrane interactions, sphingomyelin, lipid rafts, amyloid-β peptide, molecular dynamics, membrane simulations, GM1, gangliosides, peptide-ganglioside interactions

ABSTRACT

To resolve the contribution of ceramide-containing lipids to the aggregation of the amyloid-β protein into β-sheet rich toxic oligomers, we employed molecular dynamics simulations to study the effect of cholesterol-containing bilayers comprised of POPC (70% POPC, and 30% cholesterol) and physiologically relevant concentrations of sphingomyelin (SM) (30% SM, 40% POPC, and 30% cholesterol), and the GM1 ganglioside (5% GM1, 70% POPC, and 25% cholesterol). The increased bilayer rigidity provided by SM (and to a lesser degree, GM1) reduced the interactions between the SM-enriched bilayer and the N-terminus of Aβ42 (and also residues Ser26, Asn27, and Lys28), which facilitated the formation of a β-sheet in the normally disordered N-terminal region. Aβ42 remained anchored to the SM-enriched bilayer through hydrogen bonds with the side chain of Arg5. With β-sheets in the at the N and C termini, the structure of Aβ42 in the sphingomyelin-enriched bilayer most resembles β-sheet-rich structures found in higher-ordered Aβ fibrils. Conversely, when bound to a bilayer comprised of 5% GM1, the conformation remained similar to that observed in the absence of GM1, with Aβ42 only making contact with one or two GM1 molecules.

1. INTRODUCTION

Alzheimer's disease (AD) is a neurodegenerative disorder that primarily affects the elderly and is having a greater impact on societies across the globe as the overall life expectancy of humans continues to increase.[1] The exact cause of the neuronal death in AD has yet to be established, though it is widely accepted that the major contributing cause of neuronal death associated with Alzheimer's disease are toxic amyloid-β (Aβ) peptides.[2] The cleavage of the amyloid precursor protein by β- and γ- secretases results in the formation of Aβ peptides that range between 39 and 43 residues in length, of which the toxicity of the 42-residue isoform, Aβ42, is the most acute.[3]

The primary structure of Aβ42 is described in **Figure 1**.The common structural feature of Aβ peptides is an N-terminal hydrophilic region from Asp1 to Lys16, a central hydrophobic core (CHC) from Leu17 to Ala21, a central hydrophilic region from Glu22 to Gly29 and a C-terminal hydrophobic core from Ala30 to Ala42. Moreover, in spite of its high affinity for divalent cations such as Zn^{2+} and Cu^{2+}, the exact physiological role of Aβ is not known, and interestingly, Aβ can be found in monomeric form in healthy individuals at all stages of life. Monomeric Aβ can aggregate into insoluble, relatively inert, rigid structures called fibrils, but also much more toxic, soluble structures of intermediate size, and varying shapes, which are called oligomers.[4,5] Oligomers comprised mainly of Aβ42 isoform have been shown to be the most toxic.[6] Although there is a familial component to AD which suggests that elevated Aβ expression stimulates the formation of oligomers, there is evidence that suggests that factors other than expression levels causes Aβ to oligomerize.[7-9] It is thought by many that the aggregation of Aβ into toxic oligomers is *triggered*; however, this elusive trigger remains central to the understanding of Aβ toxicity, and to the possible development of an effective AD therapy.

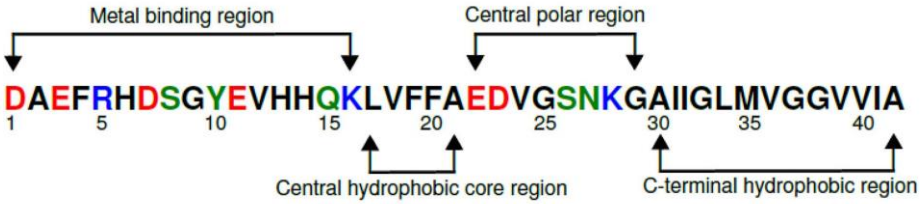

Figure 1. The primary structure of Aβ42, showing the acidic residues in red, the basic residues in blue, the hydrophobic residues in black, and the polar residues in green. The residues forming the metal binding region, the central hydrophobic core, the central polar region, and the C-terminal hydrophobic region are indicated.

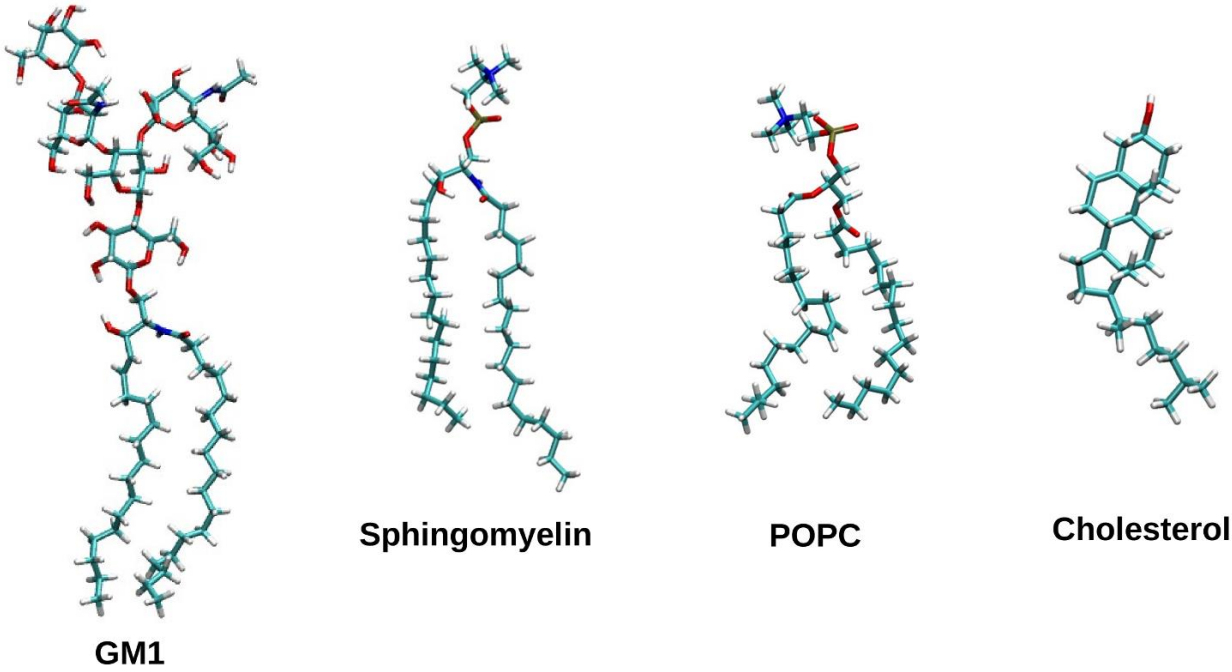

Figure 2. The structures of monosialotetrahexosylganglioside (GM1), sphingomyelin, 1-palmitoyl-2-oleoyl-phosphatidylcholine (POPC), and cholesterol used in this work.

It is becoming increasingly evident that the plasma membrane of neurons plays a role in modulating Aβ aggregation.[10-12] Moreover, the aggregation of Aβ was shown to preferentially occur in rigid liquid-ordered phases that are comprised of sphingomyelin (SM) as well as cholesterol (CHOL), which was shown to promote the interaction of the Aβ monomer with the lipid bilayer.[13-16] However, it is not known whether SM mediates Aβ aggregation through direct interactions or by altering the properties of the bilayer. The monosialotetrahexosylganglioside (GM1) has also been shown to mediate Aβ-membrane interactions,[17,18] as well as both accelerate and inhibit Aβ aggregation.[19-22] Developing a molecular understanding of how SM and GM1 affect the structure of Aβ could elucidate their role in promoting or inhibiting Aβ oligomerization.

Sphingomyelin is comprised of a phosphocholine head group, sphingosine as its backbone, and an additional fatty acid, which forms an amide bond to the amine group of sphingosine. Like sphingomyelin, GM1 also contains an amide bond between sphingosine and an additional fatty acid forms its second lipid tail; however the head group is comprised of two β-D-galactoses, one *N*-acetyl β-D-galactosamine, one β-D-glucose, and one sialic acid. The bilayers in this study will also be comprised of the ubiquitous 1-palmitoyl-2-oleoyl-phosphocholine (POPC) and cholesterol. The structures of SM, GM1, cholesterol and POPC are shown in **Figure 2**. Comparing the effects of bilayers rich in SM and those containing GM1 with bilayers comprised primarily of POPC and cholesterol will help delineate how these lipids interact with and mediate the structure of the Aβ42 peptide. This study will use molecular dynamics (MD) simulations to directly compare how these lipids affect the secondary structure of Aβ42 and the regions of the peptide that are most relevant to Aβ oligomerization. MD simulations are an indispensable complement to experimental studies providing atomistic insight into the conformational dynamics and aggregation of Aβ.[23] MD simulation studies have examined the interactions between Aβ and model bilayers of zwitterionic dipalmitoylphosphatidylcholine (DPPC) lipids and anionic dioleoylphosphatidylserine

Aβ42, sphingomyelin and the GM1 ganglioside (DOPS) lipids,[24,25] and the mutual effects of monomeric[26-28] or oligomeric[29-31] Aβ pre-embedded into different lipid bilayers, The effect of membrane lipid composition on the release of pre-embedded Aβ and Aβ oligomerization has also been investigated.[14,25,32] In this study, the MD methodology will be employed to further elucidate the role of sphingomyelin and GM1 in Alzheimer's disease.

2. METHODS

2.1 Simulated systems

In this work, bilayers comprised of POPC, SM, GM1, and cholesterol were subjected to MD simulations in the absence and presence of Aβ42. The primary structure of Aβ42 and the chemical structure of all lipids are shown in **Figures 1** and **2**, respectively. Three bilayers comprised of 288 lipids were constructed and their names and mol% compositions are as follows: 70%POPC (containing 70 mol% POPC, and 30 mol% cholesterol), 30%SM (30 mol% SM, 40 mol% POPC, and 30 mol% cholesterol), and 5%GM1 (5 mol% GM1, 70 mol% POPC, and 25 mol% cholesterol). Each bilayer was solvated by water containing 150 mM NaCl to mimic physiological conditions and to neutralize the system. The peptide-membrane systems were constructed by adding a single Aβ42 peptide and sufficient water and ions to each membrane system to solvate the peptide and to

Table 1. The Molecular composition of the three membrane systems, 70%POPC (70 mol% POPC, 30 mol% CHOL), 30%SM (30 mol% SM, 40 mol% POPC 30 mol% CHOL), and 5%GM1 (5 mol% GM1, 70 mol% POPC, 25 mol% CHOL).

Bilayer System	**Number of Molecules**							
	Peptide	**Lipids**				**Ions**		**Water**
	Aβ42	**POPC**	**CHOL**	**SM**	**GM1**	**Na^+**	**Cl^-**	
70%POPC	1	202	86	0	0	77	74	27270
30%SM	1	116	86	52	0	60	57	20841

Aβ42, sphingomyelin and the GM1 ganglioside

5%GM1	1	202	72	0	14	74	91	27121

maintain the neutral, physiological salinity of each system. Each system was simulated in a rectangular box, and the exact number of molecules contained in each system is listed in **Table 1**.

2.2 Force field

The parameters of all molecules used in this study are compatible with the OPLS-AA force field.[33,34] The original OPLS-AA parameters for cholesterol were used, and the TIP3P model was used for water.[35]

2.3 Simulation protocol

The LINCS algorithm[36] was employed to constrain the length of all bonds during the simulation to enable a 2 fs time step to be used. The isobaric-isothermal ensemble was used to keep the pressure constant at 1 bar, and scaled the box volume semi-isotropically using the Parrinello-Rahman barostat.[37] The temperature of the simulation was set to 310 K and maintained as such by using the Nosé-Hoover thermostat, with the peptide, solvent, and lipids controlled independently.[38,39] The list of non-bonded atom pairs were updated every ten simulation steps, and the Lennard-Jones interactions were cut-off at 1.0 nm. Dispersion correction was applied to both energy and pressure to reduce the dependencies on the cut-off length and to keep the model compatible with the OPLS-AA force-field. Periodic boundary conditions with the minimum-image convention were used. The electrostatic interactions were evaluated using the particle-mesh Ewald summation,[40] with an interpolation order of 6, a direct sum tolerance of 10^{-5}, and a cut-off of 1.0 nm was used for the real-space calculations. Each bilayer was simulated for at least 400 ns before the peptide was added to each system. The coordinates of the Aβ42 peptide were taken from the final frame of a previously unpublished simulation of 1 ms in water, using the same force field and solvent as was used in the current study. The Aβ42 peptide was placed approximately 5 nm above

the bilayer, as defined by the average position of the phosphorus atoms of the top leaflet. The initial secondary structure of Aβ42 was turn, except for random coil at Asp1, Ala2 and from Glu23 to Ser26, 3_{10} helix from Glu11 to Leu17, and anti-parallel β-sheet at the C-terminus from Gly33 to Ala42. All MD simulations were carried out with version 4.6.x of the GROMACS program package.[41-43]

2.4 Analysis

Each Aβ42-membrane system was simulated for three runs of 400 ns each from the same starting configuration, but with each run commencing with distinct, randomized starting velocities. 200 ns of each trajectory was analyzed using the protocol outlined below, where the starting time of the 200-ns period depends on how well the peptide adsorbed to the bilayer in each run. The data for each of the three 200 ns periods for each system was used for the analysis and quantities averaged over these three runs are presented.

2.4.1 Bilayer Properties

The membrane thickness and area per lipid (APL) averaged over the simulation time were computed using the g_lomepro program.[44] This program employs a modified version of the GridMAT-MD algorithm to map specified reference atoms onto a grid.[45] The area occupied by each lipid is quantified by summing the area of all the cells of the grid assigned to the lipid of interest, whereas the bilayer thickness is calculated by computing the difference between grid elements in the top and bottom leaflets along the vector normal to the bilayer surface (the z-axis). The phosphate atom of both POPC and SM were used as reference atoms. The deuterium order parameter, S_{CD}, provides information about the order of the acyl chains, which can be compared to values obtained from NMR experiments.[46] S_{CD}, is defined as:

$$S_{\mathrm{CD}} = \left\langle \frac{3}{2}(cos^2\theta_i) - \frac{1}{2} \right\rangle \qquad (1)$$

where θ_i is the angle between a carbon-deuterium bond (the carbon-hydrogen bond in simulations)

of the *i*-th carbon atom and the bilayer normal. The angled brackets indicate averaging over time of the relevant C-D bond in the bilayer. To determine the effect of Aβ42 on each bilayer, the order parameter was computed separately for lipids within and beyond 0.6 nm of Aβ42.

2.4.2 Bilayer-Peptide Interactions

All programs in this section are included in the standard release of the GROMACS 4.6 program package. The g_dist program was used to measure the insertion distance of Aβ42 by computing the distance between the center of mass (COM) of each Aβ42 residue and the average position of the phosphate atoms of the phospholipids taken along the z-axis. The g_contact program was used to record the number of contacts between each Aβ42 residue and each of the POPC, SM, CHOL, or GM1 lipids. A contact was recorded when the distance between any two non-hydrogen atoms from the residue and lipid in question was equal to or within 0.6 nm. The hydrogen bond propensity was determined by recording the number of times a hydrogen bond was formed between any pair of hydrogen bond donating and accepting atoms in an Aβ42 residue and any lipid type. A hydrogen bond was recorded when the angle between the hydrogen bonding donor, the hydrogen bonding hydrogen, and the hydrogen bonding acceptor was between 150^{o} and 180^{o}, and the distance between the donor and acceptor atoms was less than 0.35 nm. The g_energy program was used to compute the Coulombic and Lennard-Jones interaction energies between each Aβ42 residue and the sum of the lipids belonging to each of the POPC, GM1 and SM lipid types.

2.4.3 Aβ42 Structure

The define secondary structure program (DSSP) as implemented in the do_dssp program of GROMACS was used to assign the secondary structure to each residue of the Aβ42 peptide.[47] Due to their similarity and to facilitate a clear exposition of the data, the acquired β-strand and β-bridge data was combined and labeled β-strand/bridge, and likewise the β-turn and bend were

considered as β-turn/bend. The same method that was used to compute the hydrogen bonds between Aβ42 and the lipids in the bilayers was employed to count the hydrogen bonds within the peptide backbone the backbone and side chains, and between the side chains. Representative Aβ42 structures were obtained with the g_cluster program using the method developed by Daura et al.[48] In this method, the RMSD of the Aβ42 backbone atoms of all pairs of structures (taken from the simulation frames) were calculated and grouped based on the cutoff distance, which in this case was set to 0.25 nm and were considered as 'neighbors'. The structure with the highest number of neighbors was considered as the central structure, and all structures within the cutoff of this structure were assigned to the same cluster. The algorithm removes this cluster of structures from the remaining structures and repeats the clustering process to generate groups of non-overlapping clusters of structures with one structure at its center. The conformation and membrane interactions of the central structures of the three largest clusters for each system were rendered using the VMD program,[49] showing the position of the phosphate atoms of the simulation frame and the lipids within 6 nm of the protein.

3. RESULTS

Each trajectory was visualized as a motion picture to evaluate how the peptide adhered to the membrane. In order to evaluate and compare the mutual effect of Aβ42 and each bilayer, it was necessary to choose time windows of equal duration in each simulation where the peptide remained in contact with the bilayer. Aβ42 remained in continuous contact with the each bilayer for at least 200 ns In the case of the 70%POPC and 5%GM1 trajectories the peptide adhered to the bilayer readily, therefore the last 200 ns of each run was selected. In the case of the third run of the 30%SM bilayer, Aβ42 lost contact with the bilayer after 300 ns, therefore the analysis period was between 80 ns and 280 ns. Thus, Aβ42 was in contact with each bilayer for the duration of each trajectory analysis time period.

3.1 Effect of Aβ42 on Bilayer Properties

The following sections describe the properties of the three bilayers investigated in this study, 70%POPC (comprised of 70% POPC, and 30% CHOL), 30%SM (30% SM, 40% POPC, and 30% CHOL), and 5%GM1 (5% GM1, 70% POPC, and 25% CHOL).

3.1.1 Area Per Lipid and Bilayer Thickness

The area per lipid of the 70%POPC, 30%SM and 5%GM1 bilayers ranged from 0.64-0.78 nm^2, 0.65-0.80 nm^2, and 0.58-0.77 nm^2, respectively. As shown in **Figure 3**, each bilayer was undulated and contained regions with high and low APL values in relatively close proximity. Such undulations were not present in the bilayers before the addition of Aβ42, which suggests that the undulations were caused by interactions between peptide and bilayer. The APL values between leaflets were not correlated, which means that the higher APL values on one leaflet did not in every case correspond to lower (for a negative correlation) APL values on the same region of the lower leaflet. The ranges in thickness of the three bilayers were as follows: 70%POPC (4.34-4.56 nm), 30%SM (4.36-4.60 nm) and 5% GM1 (4.44-4.74 nm) and the bilayer thickness was less affected by the undulations than the APL values were. The temporal behavior of the bilayer thickness has been computed for each system and shown in **Figure S1**. This demonstrated that the Aβ42 monomer did not affect the thickness of the bilayer during any of the simulation runs.

3.1.2 Order Parameter

As shown in **Figure 4**, the sn-1 tail of POPC in the 70%POPC bilayer was the most ordered at C8 (0.328 S_{CD}), whereas the sn-2 tail was the most ordered at C5 (0.273 S_{CD}). There was a negligible difference between the order parameters when the peptide was greater than 0.6 nm from the lipids as when they were less than 0.6 nm. The order of the POPC tails increased by 0.02 S_{CD} in the 30%SM bilayer. Moreover, the SM lipids were more ordered than the POPC lipids were in this bilayer. Conversely, the order of the POPC tails decreased in the 5%GM1 bilayer and in this bilayer the GM1 tails were more ordered than POPC tails were. In the 30%SM bilayer the tails of the lipids

Aβ42, sphingomyelin and the GM1 ganglioside

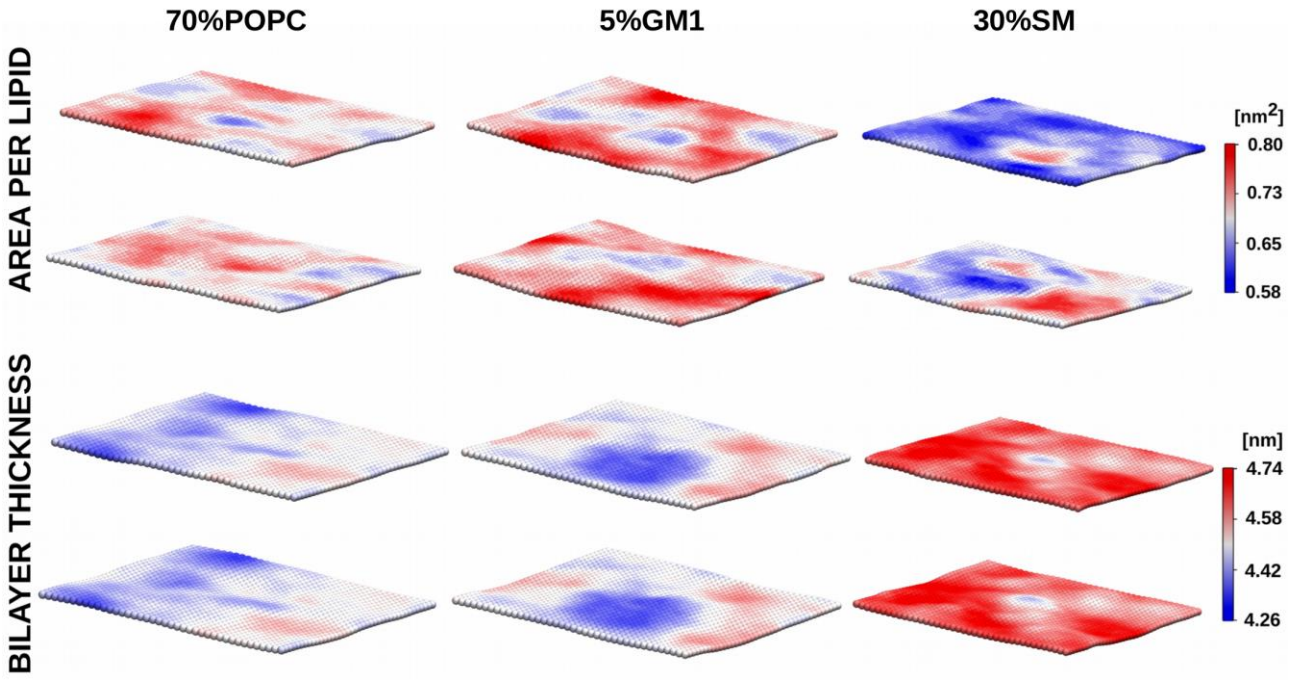

Figure 3. The average area per lipid (APL) and bilayer thickness of each bilayer whilst interacting with Aβ42.

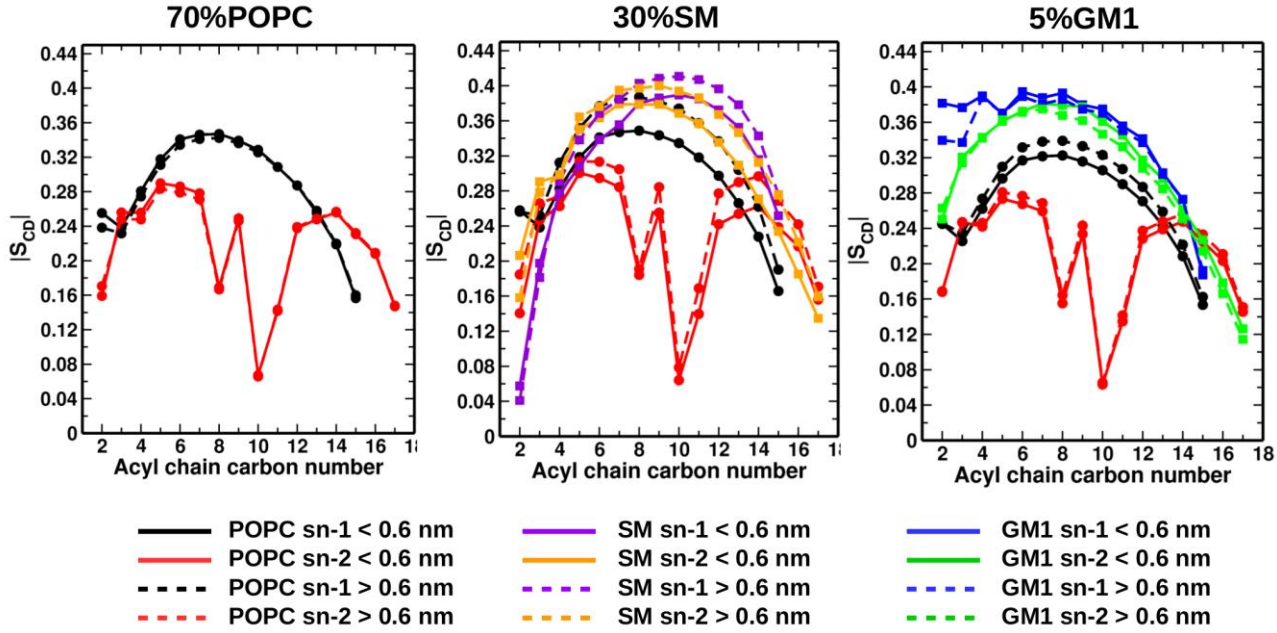

Figure 4. The order parameter of the acyl chains of each lipid in the bilayer systems that is closer than and further than 0.6 nm from the Aβ42 peptide.

Aβ42, sphingomyelin and the GM1 ganglioside within 0.6 nm of Aβ42 were less ordered than those greater than 0.6 nm away from Aβ42, and the peptide disordered the POPC lipids more than it did SM lipids in this system. Aβ42 also disordered the POPC tails in the 5%GM1 bilayer, but this effect was less than that observed for POPC in the 30%SM bilayer. Aβ42 increased the order of the GM1 tails, but this effect was almost negligible.

3.2 Effect of Bilayer on Aβ42

3.2.1 Aβ42 Insertion Distance

In order to see how Aβ42 associates with the bilayers, we calculated the insertion distance of the peptide residues as their average position along the vector parallel to the bilayer normal (z-axis), where the average position of the phosphorus atom of the phosphate group of POPC was used as a reference point. In all three bilayers, the hydroxyl oxygen of cholesterol laid approximately 0.5 nm beneath the phosphate group of POPC, as shown in **Figure 5**. Despite having identical head groups, the phosphate group of sphingomyelin laid approximately 0.1 nm above that of POPC in the 30%SM bilayer. On average, the center of mass of the GM1 head group was approximately 0.5 nm above the phosphate group of POPC.

In the 70%POPC and 5%GM1 bilayers the Asp1 residue is closest to the average position of the phosphate atom of the POPC lipid, which was used as a reference point, though it was approximately 0.5 nm above both bilayers. Similarly in both bilayers, the residues in the central polar region (Ser26 to Lys28) were the next closest. The central two residues at the center of the C-terminal hydrophobic region, Val36 and Gly37, were the furthest from the bilayer, followed by the residues at the central hydrophobic core (Leu17 to Ala21). The main difference between the 70%POPC and 5%GM1 bilayers is that the Aβ42 stays slightly closer to the 70%POPC membrane than it does to the 5%GM1 bilayer. Aβ42 stays further away from the 30%SM bilayer than it does from the 70%POPC and 5%GM1 bilayers, and this more pronounced at residues Ser26 to Lys28 in the central polar region. In the case of the 30%SM bilayer, the C-terminal segment of the C-

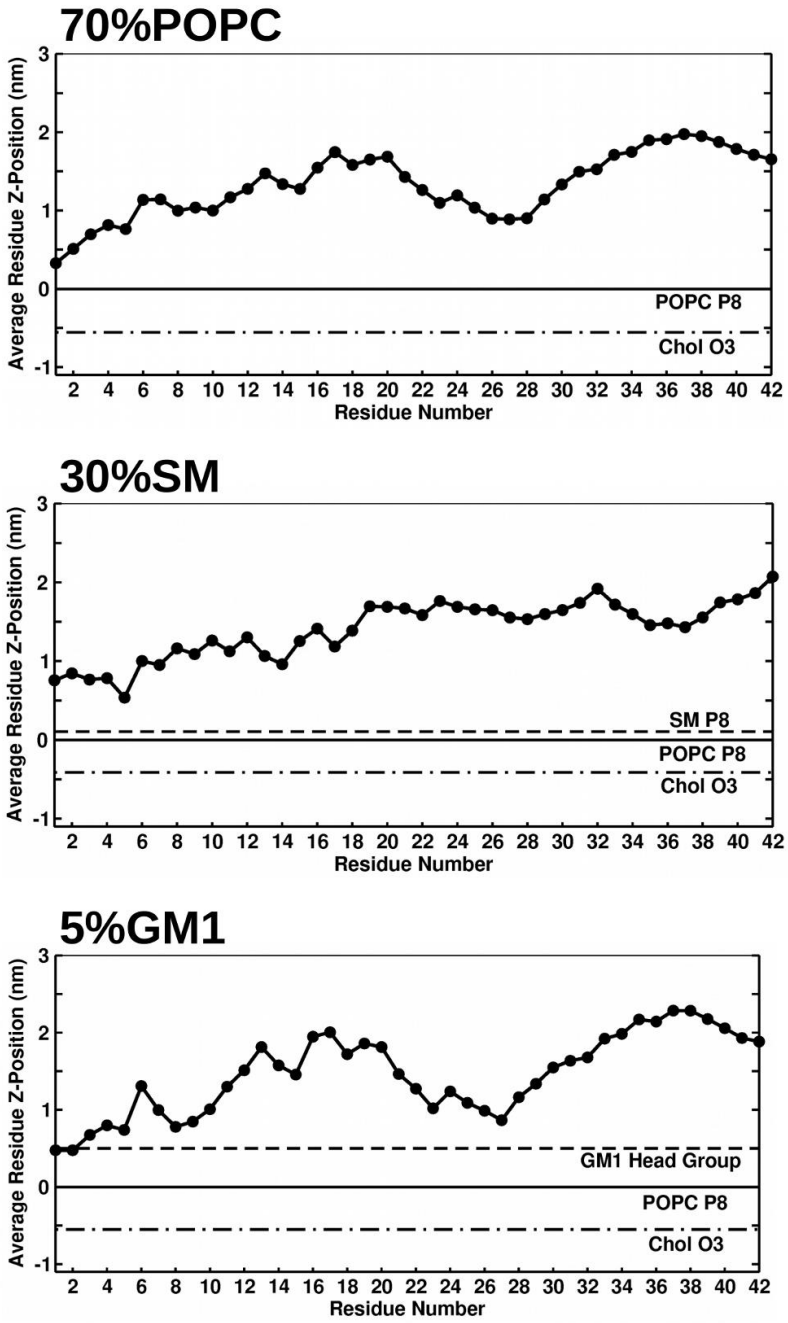

Figure 5. The average insertion distance of each Aβ42 residue between Aβ42 and the 70%POPC (70% POPC, and 30% CHOL), 30%SM (30% SM, 40% POPC, and 30% CHOL), and 5%GM1 (5% GM1, 70% POPC, and 25% CHOL) bilayers.

Aβ42, sphingomyelin and the GM1 ganglioside terminal hydrophobic region is the furthest from the bilayer instead of the central residues of this region as in the other two bilayers.

3.2.2 Aβ42 Contacts and Hydrogen Bonds with Bilayers

For obtaining a more detailed understanding which Aβ42 residues associated with the bilayers, we calculated the average number of contacts over the three runs between each residue and the different lipid types. On average, the N-terminal residues of Aβ42 made the most contacts with the 70%POPC bilayer (**Figure 6**). In this region the most contacts were made with Asp1 (75.5 contacts) and Arg5 (45.8 contacts) and 25 to 45 contacts were made with the residues in between. In this region the next highest peak was at Tyr10, though very few contacts were made at Asp7 and Glu11. Fewer than 10 contacts were made between the 70%POPC bilayer and the central hydrophobic core, and similarly low numbers were obtained at the C-terminal hydrophobic region. The contacts made in the central polar region generally increased from Glu22 (11.7 contacts) to Lys28 (44.9 contacts). Contacts were made with cholesterol only in the 70%POPC bilayer and only in one of the three runs at Asn27 (6 contacts) and Ser26 (2 contacts), but this data is not shown. This is because the hydroxyl group of cholesterol was below the phosphate atom of POPC, which largely prevented Aβ42 from making contacts with cholesterol. Conversely, almost no contacts were made between the central polar region of Aβ42 and the 30%SM bilayer, as shown in **Figure 6**. The majority of the contacts were made between the N-terminal region of Aβ42 and the 30%SM bilayer, although the distribution of the Aβ42 residues that made contact with the POPC lipids differed from the distribution of residues that made contacts with the SM lipids. Asp1 and Arg5 of Aβ42 made the most contacts with the 30%SM bilayer, but Arg5 made more contacts with the phosphocholine of sphingomyelin than that of the POPC lipids. In the 5%GM1 bilayer, the distribution of the Aβ42 residues that made contact with POPC was similar to that observed in the absence of GM1. There, a

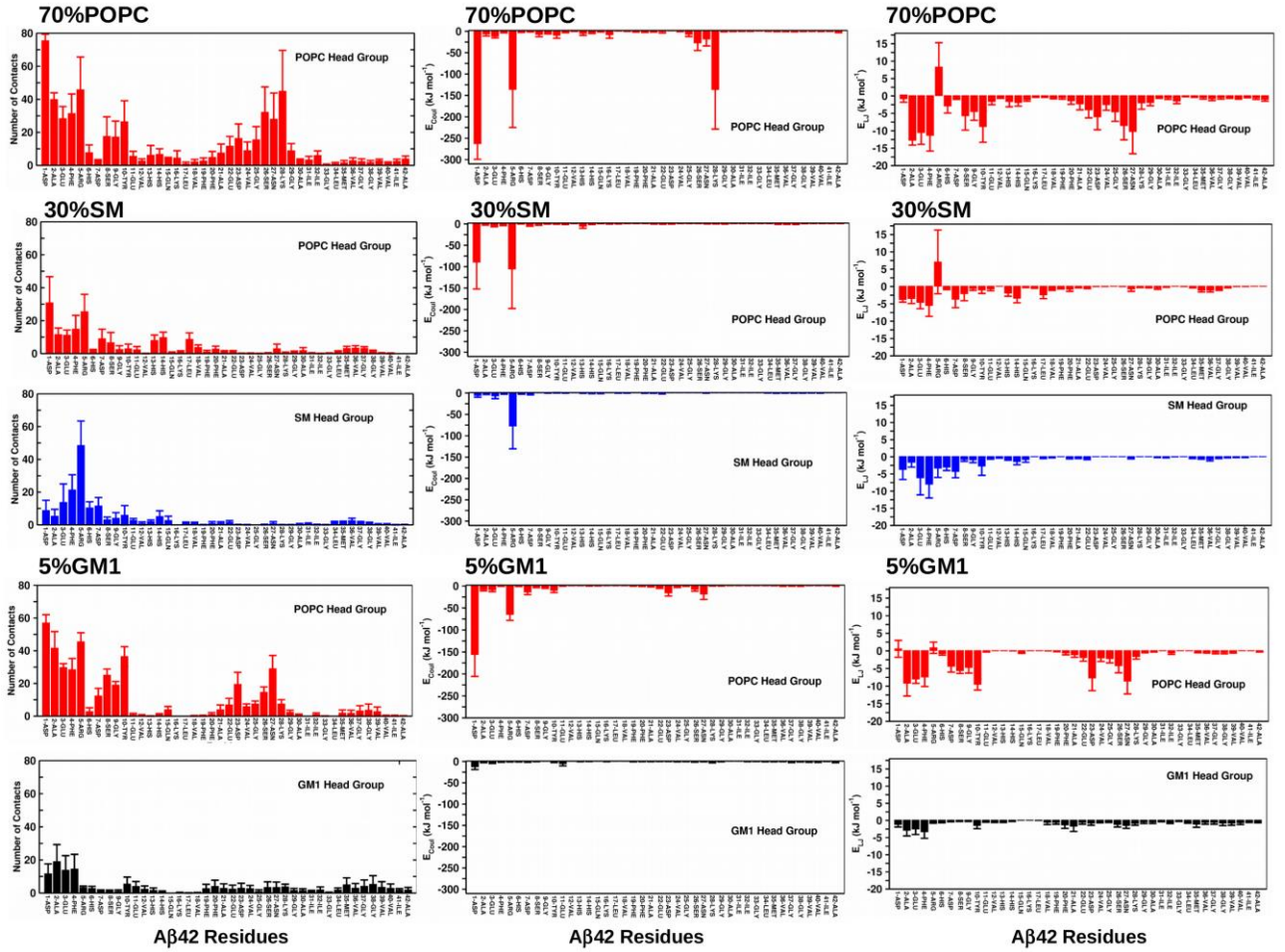

Figure 6. The average number of contacts (left), Coulombic (center), and Lennard-Jones energies (right) of each Aβ42 residue (and standard error of the mean) between Aβ42 and the 70%POPC (70% POPC, and 30% CHOL), 30%SM (30% SM, 40% POPC, and 30% CHOL), and 5%GM1 (5% GM1, 70% POPC, and 25% CHOL) bilayers.

reduced number of contacts were made at the central polar region of Aβ42 (Glu22-Lys28) compared to those made in the N-terminal region. Between ten and twenty contacts per residue were made between the GM1 lipid and residues Asp1 to Phe4 of Aβ42. Less than five contacts were made between each of the remaining residues and GM1, but GM1 made contacts with more Aβ42 residues than POPC or SM did.

Asp1 and Arg5 in the N-terminal metal binding region, as well as Ser26, Asn27 and Lys28 in the central polar region formed hydrogen bonds with POPC in the 70%POPC bilayer, as shown in **Table S1**. The hydrogen bond propensities were higher in the N-terminal region of Aβ42 (75% in Asp1 and 50% in Arg5) than in the central polar region, which displayed hydrogen bond propensities of 20%-50%. When the sum of POPC and SM lipids were considered, the hydrogen bonding propensities of Asp1 and Arg5 in the 30%SM bilayer increased compared to their propensities in the 70%POPC bilayer, whereas quite alarmingly, no hydrogen bonds formed between these lipids and the residues of the central polar region. In the 5%GM1 bilayer, the N-terminal residues had similar hydrogen bond propensities compared to the hydrogen bonding propensities of these residues in the presence of the 70%POPC bilayer, whereas, similar to what was seen in the case of 30%SM, the hydrogen bonding propensities of the central polar residues in the presence of the 5%GM1 bilayer were greatly reduced (**Table S1**). GM1 showed a low hydrogen bond propensity (10% or less) with Aβ42 residues, however GM1 was the only lipid that formed hydrogen bonds with residues in the C-terminal hydrophobic and central hydrophobic regions of Aβ42.

3.2.3 Aβ42-bilayer Interaction Energies

Next, we analyzed whether the contacts between Aβ42 and the lipid bilayers were driven by electrostatic or Lennard-Jones (LJ) interactions. The strongest contributions to the Coulombic interaction energy (**Figure 6**) between the POPC residues in the 70%POPC bilayer were Asp1 at

–260 kJ·mol^{-1}, whereas the interaction strength was approximately half that value at the next strongest interacting residues, Arg5 and Lys28. The Coulombic energy between Aβ42 and POPC in the 30%SM bilayer was one-third the strength it was in the 70%POPC bilayer at Asp1 and three-quarters the strength it was at Arg5, whereas it was close to zero between Asn27 and both the POPC and SM lipids in the 30%SM bilayer. The Coulombic energy between Asp1 and SM was also near zero in the 30%SM bilayer. In the 5%GM1 bilayer the distributions of the Coulombic energies between the Aβ42 residues and POPC lipids were similar to those in the 70%POPC bilayer but were lower in magnitude. Surprisingly, the magnitude of the attractive Coulombic interaction energies between the Aβ42 residues and the GM1 lipids were low, with no single residue averaging an interaction energy greater than 20 kJ·mol^{-1}.

The profile of the LJ interaction energies between Aβ42 and the lipids of each bilayer were very similar to that of their respective contact map (**Figure 6**). In the 70%POPC bilayer the strongest LJ interactions were between the POPC lipids and the metal binding region and central polar regions of Aβ42, particularly residues Ala2-Phe4, Tyr10, Asp23 and Asn27, which, with the exception of Tyr10 and Asp23, had LJ energies that averaged between –10 and –15 kJ·mol^{-1}. In the 30%SM bilayer, the interacting residues were similar except for those in the central polar region, Glu22 to Gly29, which had energies close to zero. The sum of the attractive interaction energies of both POPC and SM lipids with each of the remaining Aβ42 residues was less than the attractive interaction energies between the residues that interacted with the POPC lipids in the 70%POPC bilayer (both bilayers had the same number of phosphocholine head groups). Interestingly, for Arg5 the repulsive contributions to the Lennard-Jones potential were higher than the magnitude of the attractive van der Waals interactions, leading to positive interaction energies with POPC lipids in both bilayers but not with SM in the 30%SM bilayer. However, these positive values are more than compensated by the electrostatic attraction between Arg5 and POPC. The Aβ42 residues that

Aβ42, sphingomyelin and the GM1 ganglioside interacted with POPC in the 5%GM1 bilayer were similar to those that interacted with POPC in the 70%POPC bilayer, however the respective magnitudes were slightly lower. As in the contact maps, the residues with the strongest LJ interactions were in the N-terminal region. The strength of the interactions with the remaining residues was quite low, at around –2 to –3 $kJ \cdot mol^{-1}$.

3.3 Aβ42 Structural Properties

The following sections describe the structure of the Aβ42 peptide whilst interacting with each bilayer.

3.3.1 Aβ42 Secondary Structure Assignments

In the 70%POPC bilayer, residues Asp1 and Ala2 were always disordered, as shown in **Figure 7**. Residues Glu3 to Tyr10 displayed a mixture of disorder and turn, residues Glu11 through Ala21 displayed a mixture of β-turn/bend and helix (with disorder from Glu11 to His13), residues Glu22 to Ile33 displayed a mixture of disorder and β-turn/bend (with some β-strand/bridge), whereas residues Gly33 to Ala42 were a mixture of random coil, β-strand/bridge, and β-turn/bend. Apart from the helices, there were residues in these regions that were almost always (with a probability close to 1) assigned the same secondary structure. The most interesting structure was the prevalence of the β-strand/bridge of Met35 and Val40. In the helical region residues Glu11 to Leu17 were primarily α-helical, whereas residues Val18 to Glu22 were primarily 3_{10}-helical. When interacting with the 30%SM bilayer the regions that were helical in the presence of 70%POPC were more β-turn/bend-like, and the β-turn/bend that centered on Gly25 in 70%POPC was converted to a random coil in 30%SM. Interestingly, only when Aβ42 interacted with the 30%SM bilayer a β-strand/bridge was observed at the N-terminus, with strong prominence at Arg5 (0.68 probability) and Tyr10 (0.78 probability). Similar to what was seen in 70%POPC, whilst interacting with the

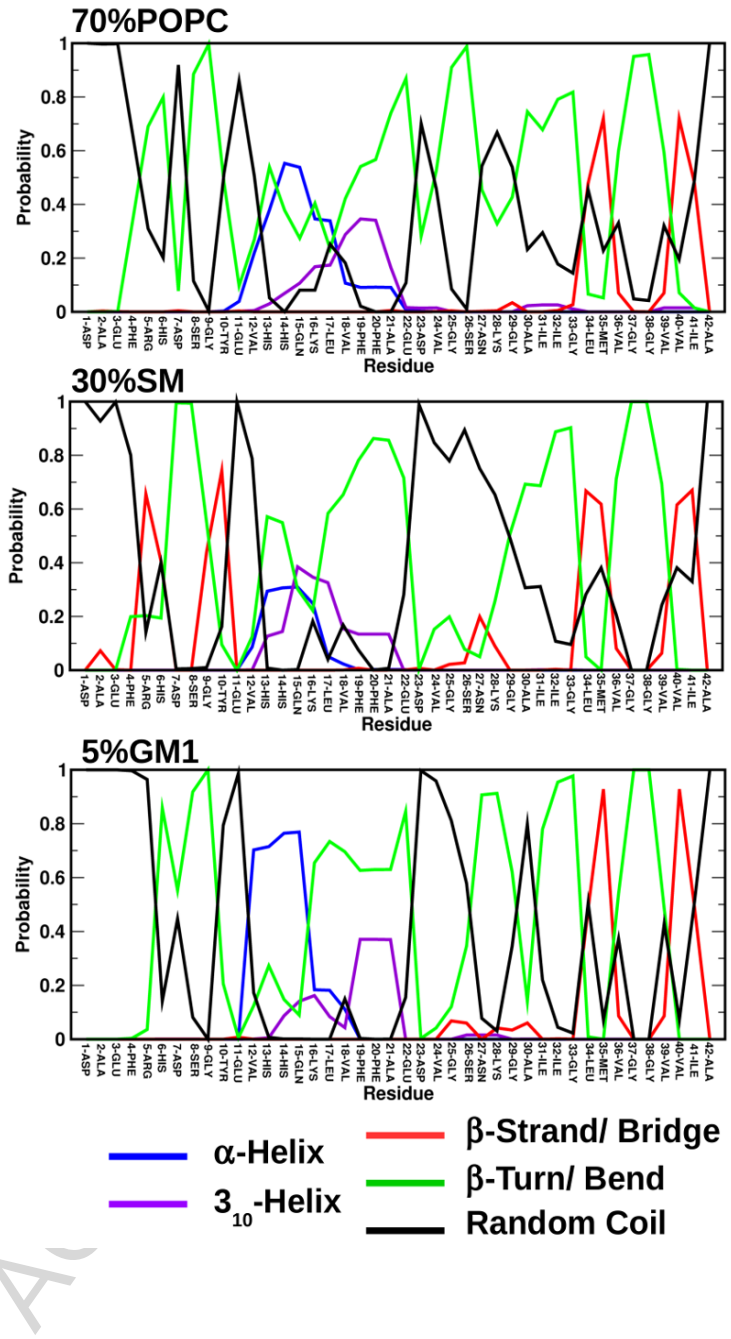

Figure 7. The secondary structure assignment of each Aβ42 residue in the presence of each the 70%POPC (70% POPC, and 30% CHOL), 30%SM (30% SM, 40% POPC, and 30% CHOL), and 5%GM1 (5% GM1, 70% POPC, and 25% CHOL) bilayers.

Aβ42, sphingomyelin and the GM1 ganglioside GM1 bilayer the β-sheet at the N-terminus was a random coil and β-turn/bend, however the propensity of the β-sheet at the C-terminus was higher in 5%GM1 than it was in the other two bilayers. Apart from an increase in helicity in 5%GM1, the secondary structures in the remaining regions of Aβ42 were similar to what they were in the in the 70%POPC bilayer.

3.3.2 Aβ42 Intramolecular Hydrogen Bonds

Hydrogen bonds present within the peptide backbone, between backbone and peptide side chain, and between side chains that were present more than 40% of the time were recorded and tabulated in **Table S1**. In 70%POPC backbone to backbone hydrogen bonds were present between Val18 and His14, Ala21, and Glu22. In the C-terminal region hydrogen bonds were present between Gly33 and Ile41, Val36 and Val39, and Ile41 and Leu34, which stabilized a β-sheet structure. Glu3 and Asp7 were the two main hydrogen bond acceptors whereas peptide bonds in the N-terminal region, such as the backbone of Phe4 and Arg5 and the side chain of Arg5, acted as donors. Almost all of the these hydrogen bonds were present in 30%SM and 5%GM1 bilayers, however these systems caused backbone to backbone hydrogen bonds to form between additional residue pairs, and within the Aβ42 backbone in particular. These additional bonds were between residues that either formed helices or β-sheets that were not fully formed, and such structures are discussed in the next section about the Most Prevalent Aβ42 Structures. Residues in the N-terminal region (Tyr10-Lys16) of Aβ42 did not form backbone to backbone hydrogen bonds in 70%POPC but did so in both 30%SM and 70%POPC. The hydrogen bonds involving Aβ42 side chains in the 30%SM and 5%GM1 bilayers were largely similar to the ones present when Aβ42 was in the 70%POPC bilayer, as shown in **Table S1**. However there were additional side chain to side chain hydrogen bonds between Gln15 and Glu22 and Lys28 and Glu11 in the 5% GM1 bilayer.

3.3.3 The Most Prevalent Aβ42 Structures at Each Bilayer

The three highest populated Aβ42 clusters found in the 70%POPC bilayer represented 9.5%, 8.0%, and 6.6% of all structures, respectively. The central structure in each cluster denoted as Structures 1-3 from the largest cluster to third-largest cluster, are shown in **Figure 8**. From the N-terminus to C-terminus, the secondary structure of each structure alternated from random coil to turn, followed by a helical region, a turn region and an anti-parallel β-sheet (on either side of a turn) at the C-terminus. The N terminus was embedded into the bilayer, as was a turn centered on Asn27, in each of the three most prevalent structures. However the N-terminus was the least embedded in Structure 2, whereas the Asn27 was the least embedded in Structure 1. The three most populated Aβ42 structures found in the 30%SM bilayer represented 38.9%, 16.5%, and 9.9% of all structures, respectively, as shown in **Figure 9**. There were no helices in Structure 2, and no β-sheet in Structure 3. In lieu of β-sheets, Structure 3 did have β-bridges at the N and C termini. A much higher β-sheet content was found in Structure 2, as β-sheets were observed in both termini, with Lys28 forming a β-bridge to the β-sheet in the N-terminus. Moreover, a β-bridge was present in the N-terminal region in Structure 1 in additional to the β-sheet at the C-terminus. Although there were no β-sheets in the N-terminal region of Structures 1 and 3, there were hydrogen bonds within the backbone that seemed to support a β-sheet-like structure in this region. Only the N-terminus of Structure 2 is embedded into the 30%SM bilayer, whereas neither Asn27 nor any other residue embeds itself into the 30%SM bilayer in any of the three most prevalent Aβ42 structures, which has already been revealed by the contact map in **Figure 6**. In the presence of 5%GM1 (**Figure 10**), the three largest Aβ42 clusters represented 33.2%, 31.4%, and 11.1% of the total number of structures, which shows that GM1 even more strongly reduced the conformational flexibility of Aβ42 than SM did. Even though Aβ42 was within 0.6 nm of only two GM1 lipids in Structure 1 and within one GM1

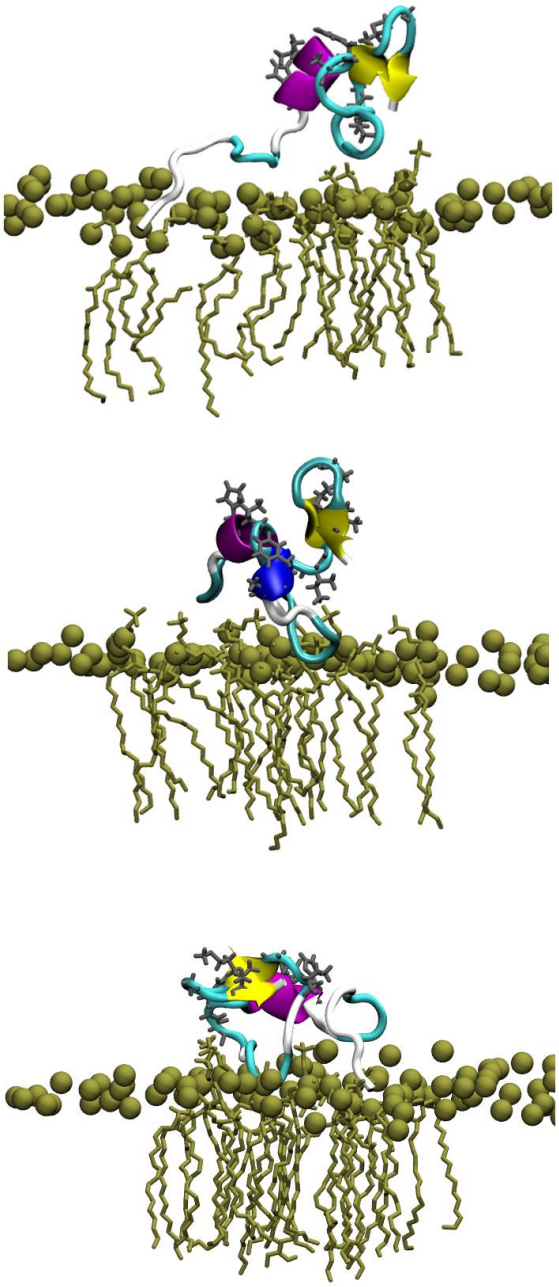

Figure 8. The central Aβ42 structure of the three largest clusters in the 70%POPC bilayer (70% POPC, and 30% CHOL), where the largest to smallest cluster is shown from top to bottom. In each rendered image the Aβ42 peptide is coloured by secondary structure element, with turn shown in cyan, α-helix shown in blue, 3_{10}-helix shown in purple, β-sheet shown in yellow, and random coil shown in white. The residues engaged in backbone to backbone hydrogen bonds (from Table S1) are shown in grey. The phosphate atom of each POPC lipid is shown as a tan sphere, whereas the lipids within 0.6 nm of Aβ42 are shown in a tan-coloured, licorice representation.

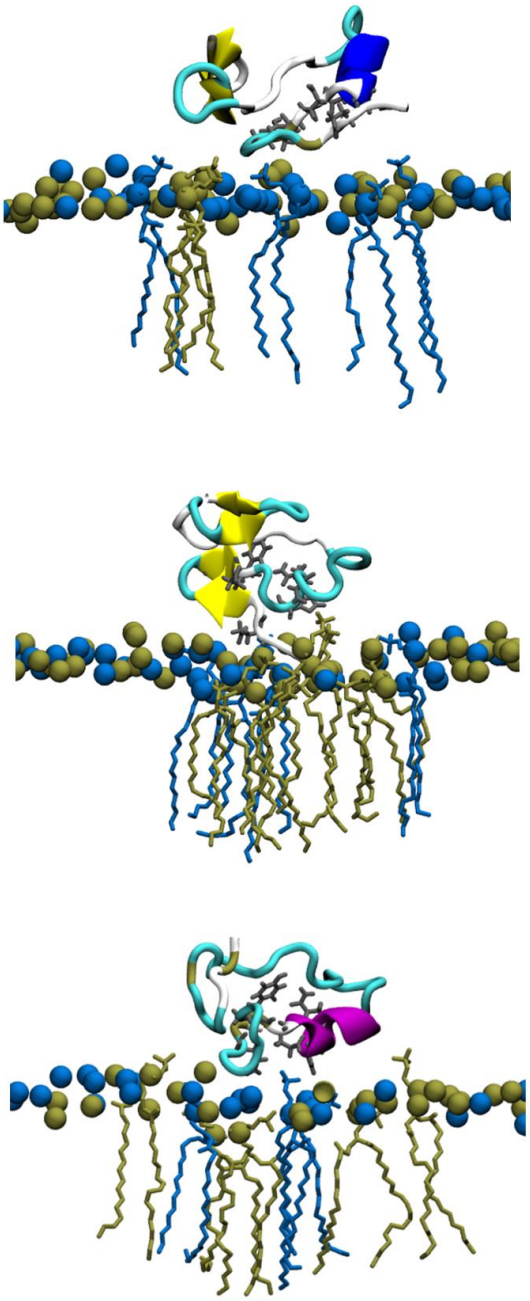

Figure 9. The central Aβ42 structure of the three largest clusters in the 30%SM bilayer (30% SM, 40% POPC, and 30% CHOL), where the largest to smallest cluster is shown from top to bottom. In each rendered image the SM lipids are shown in blue. See **Figure 8** for an explanation of the other coloring.

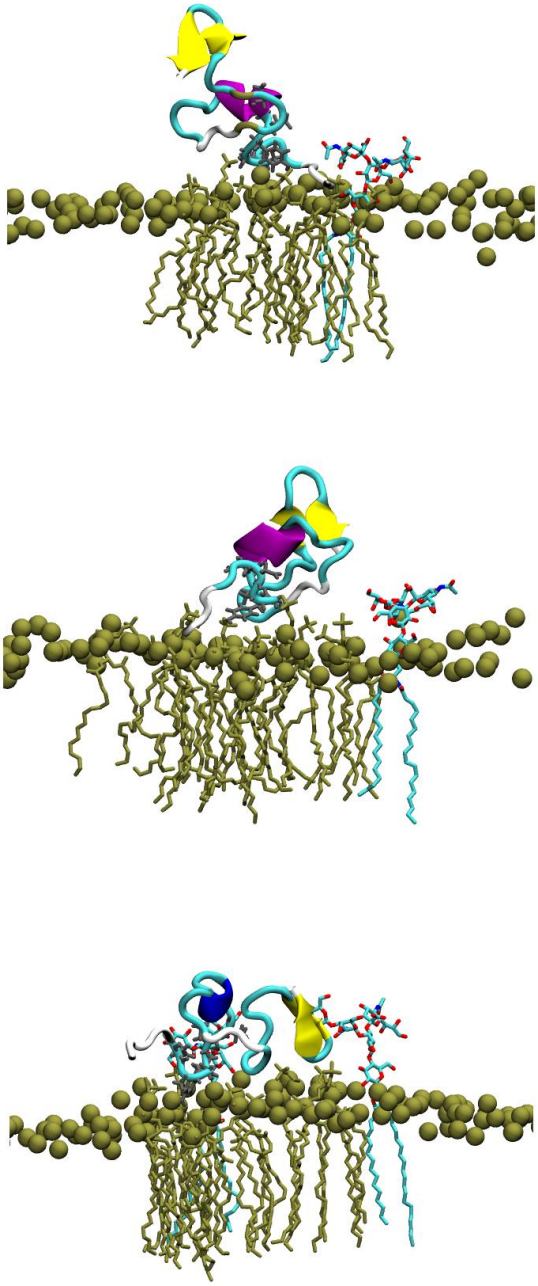

Figure 10. The central Aβ42 structure of the three largest clusters in the 5%GM1 bilayer (5% GM1, 70% POPC, and 25% CHOL), where the largest to smallest cluster is shown from top to bottom. In each rendered image GM1 is shown colored by atom, with carbon coloured in cyan, oxygen in red, and nitrogen in blue. See **Figure 8** for an explanation of the other colouring.

Aβ42, sphingomyelin and the GM1 ganglioside structure in each of Structures 2 and 3. As was seen in the 70%POPC bilayer, Aβ42 contained random coil, turn, helices and a C-terminal β-sheet, however, a higher degree of turn was present in place of random coil. The N-terminus was embedded into the 5%GM1 bilayer in Structure 2 but not in Structures 1 and 3, however in Structure 1 the N-terminal region was closely associated with the bilayer. In Structures 2 and 3, turns centered on Gly9 and Lys28 interacted with the bilayer, whereas only in Structure 3 did a turn centered on Val39 interact with the bilayer.

4. DISCUSSION

4.1 Sphingomyelin Affects Aβ42 Conformation by Changing the Bilayer Properties

The lack of correlation of the APL values between the leaflets (where higher APL values on one leaflet correspond to lower APL values on the other leaflet),[50] as well as the lack of correlation between bilayer thickness and APL (where lower thickness values in one region correspond to higher APL values in the same region) suggests that Aβ42 had an effect on the bilayer structures. The effect of the Aβ42 on the order parameter was small, as shown by the order parameter values determined for the lipids within 0.6 nm of Aβ42 and those beyond 0.6 nm of Aβ42 (**Figure 4**). The insertion and contact data indicated that Aβ42 almost exclusively interacted with the phosphatidylcholine head groups, with almost no contacts made with cholesterol, which lay lower beneath the phosphate groups. Interestingly, the interaction of Aβ42 with the phosphatidylcholine head group of POPC had almost no effect on the order of the acyl chains of POPC, while on the other hand, interactions between Aβ42 and SM disordered the acyl chains of SM. This effect was also observed in GM1 to a lesser degree. The interactions between Aβ42 and the bilayers occurred preferentially at the N-terminus (Asp1) and at a turn which centered on Asn27, which also involved Ser26 and Lys28. As shown in the most prominent structures and the average insertion distance (**Figure 5**), these residues more strongly inserted into the bilayers in the order of 70%POPC > 5%GM1 > 30%SM.

The observation that Aβ42 disorders the lipids in the 30%SM and (to a lesser degree) those in 5%GM1 can perhaps be attributed to the rigidity of the ceramide-containing SM and GM1 lipids. Ceramides contain an amide group, a free hydroxyl on C3, and a double bond between C4 and C5. The amide N-H and hydroxyl group can act as both hydrogen bond donors and acceptors, whereas the amide oxygen can also act as a hydrogen bond acceptor. On the other hand, the ester carbonyls in POPC can only act as donors.[51] These hydrogen bonds increase the rigidity of the lipids and consequently the bilayers the lipids comprise. POPC remains quite fluid, and the movement of the head group facilitates interactions between lipid and peptide with little to no effect on the order of the POPC lipid tails. Comparatively, SM is more rigid, with its phosphatidylcholine forming fewer hydrogen bonding interactions with Aβ42 (**Figure S2**). The effects of Aβ42 binding are transferred along the more rigid SM, both disordering the SM lipid tails and affecting the POPC tails in 30%SM by direct contact. The effect of the increased rigidity of the bilayers comprised of increasing amount of sphingosine-containing lipids, on the peptide-bilayer interactions are discussed below.

4.2 Changing Bilayer Properties Affect Peptide-Bilayer Contacts and Interaction Energies

The effect of the bilayer type on their interactions with Asp1, and Ser26, Asn27, and Lys28 are also shown quantitatively in the peptide-bilayer contacts, as contacts between the lipids in each respective bilayer and the Aβ42 residues at the N-terminus and near Asn27 are formed in the order of 70%POPC > 5%GM1 > 30%SM. **Figure S2** demonstrated that these contacts were driven by the hydrogen bonds that formed between amino acid residues and lipids. It is in the hydrogen bonding interactions that the differences between the lipids in the bilayers are the most telling. A hydrogen bonding propensity of near 40% between residues Ser26, Asn27, and Lys28 and POPC in the 70%POPC bilayer is completely abolished in both POPC and SM in the 30%SM bilayer, and reduced to less than 10% and to only Ser26 in 5%GM1. Interestingly, this hydrogen

bonding disparity is in spite of the fact that each bilayer contains the same amount of lipids with the phosphatidylcholine head group (70%), since the head groups of POPC and SM are identical. A likely reason why the central hydrophobic region of Aβ42 fails to form hydrogen bonds in the 30%SM bilayer and nearly so in 5%GM1 could be related to the inability of Aβ42 to insert into the more rigid 30%SM bilayer. Hydrogen bonds did form between Asp1 and Arg5 (side chain) of Aβ42 with residues in all three bilayers.

Not surprisingly, the Aβ42 residues that formed hydrogen bonds with the respective bilayers were also shown to be the strongest energetic contributors to the interactions between Aβ42 and each bilayer. The interactions between each Aβ42 residue and the bilayers were divided into their Coulombic and Lennard-Jones contributions. Overall, the Coulombic interactions dominated, since the magnitude of Coulombic interactions were on average 10-fold stronger than the Lennard-Jones interactions at each residue. The disparity between energy types is such that Arg5 displayed an unfavorable Lennard-Jones interaction with POPC in both 70%POPC and 30%SM, and still maintained a large number of contacts with these bilayers due to the much more favorable Coulombic interactions. There were strong Coulombic interactions between the N-terminal region (Asp1 and Arg5) and the central polar region (primarily Asn27) and the bilayers in the order of 70%POPC > 5%GM1 > 30%SM. The distribution of the Lennard-Jones energies per residue between bilayers was also in that order, however they more resembled the distribution of the contacts.

Aβ42 made far fewer contacts, hydrogen bonds and had much weaker interactions with GM as compared to its interactions with the phosphatidylcholine head group of POPC and SM1. In spite of its much larger head group, at a lipid concentration of 5%, only seven GM1 lipids were present in each leaflet, compared to 202 PC head groups. Thus, the PC head groups created a much larger surface area for interactions with Aβ42. As shown in the representative structures in

5%GM1, Aβ42 still interacted strongly with the PC lipids even with GM1 present. In the three representative Aβ42-5%GM1 structures, Aβ42 only had one or two GM1 molecules within 0.6 nm. These relatively distant interactions, also supported by the sparse number of contacts, and low Aβ42-GM1 interaction energies, are possible reasons why the Aβ42-5%GM1 interactions had a minimal effect on the conformation of Aβ42 compared to the effect that the Aβ42-30%SM interactions did.

4.3 Altered Bilayer Properties Affect Aβ42 Secondary Structure

The secondary structure of Aβ42 had some similar secondary structure elements in each bilayer, particularly in the C-terminal β-sheet region (Gly33 to Ala42) and the helical central polar region (Val12 to Glu22). As evinced by the contacts, hydrogen bonding, and interaction energies, the conformation of Aβ42 in the N-terminal regions and central polar regions were affected by interactions with the bilayers. The strong interactions between Asn27 and the POPC lipids in the 70%POPC and 5%GM1 bilayers stabilized the formation of a turn, where, due to the lack of interactions with the SM bilayer these residues maintained a random coil. Moreover, at the N-terminus, Asp1 was able to form hydrogen bonds with POPC in the 70%POPC and the 5%GM1 bilayers but not so much with the 30%SM bilayer. This could be the reason why an N-terminal β-sheet was able to form in the 30%SM bilayer, but not in the other two systems. This is a very interesting observation, given the toxicity of Aβ42 is related to a conformational change into a β-sheet-rich state.[52] This β-sheet shown in the assignment of residue secondary structure plot in **Figure 7**, whereas the lack of insertion is shown in the representative plots in **Figure 12**, as well as the absence of hydrogen bonds between Asp1 and POPC. Though the β-sheets are more pronounced in Structure 2 in the 30%SM bilayer, the intrapeptide, backbone to backbone hydrogen bonds indicate a structure very similar to that of a β-sheet in the other two largest clusters. The S-shaped β-sheet rich-structures observed in 30%SM are very similar to recently obtained structures of Aβ

Aβ42, sphingomyelin and the GM1 ganglioside fibrils derived from NMR[53-56] or cryo-EM[57] and oligomers reviewed by Nagel-Steger et al.[5] By fixing the N-terminus to the membrane, the other two bilayers still show potential for Aβ assembly by constraining the N-terminus, which is the most flexible region of the Aβ42 peptide.

4.4 Comparisons with other Studies

MD simulations complement other experimental approaches by providing an atomistic view of the system under investigation. In this study the specific interactions that affect how Aβ interacts with different bilayers affect its conformation in ways that could promote its formation into toxic oligomers. One limitation of the MD technique is the limitations on system size and system complexity. This could hamper the ability to study systems that would include mixtures of larger oligomers, and the effects on bilayer structures on a time scale that could induce pore formation. Nevertheless an atomistic description of the interactions between the Aβ42 monomer and three bilayer types is presented in this study. The secondary structure of Aβ peptide is known to be intrinsically disordered and to contain a mixture of secondary structures, both in experiment and simulations.[23,53,58,59] The C-terminal β-sheet observed in this study has been proposed to be the nucleation site that promotes the aggregation of Aβ into β-sheet-rich structures.[60,61] In this study Ile41 and Asp42 form the C-terminal β-sheet, which is not stable in the less aggregation-prone Aβ40 due to the absence of these residues. Experimental studies have shown that Aβ interacts strongly with bilayers comprised of the phosphatidylcholine head group,[62,63] and that electrostatic forces yield the association of Aβ to phospholipid membranes. The results of our work highlight that this interaction is mediated by hydrogen bonds with Arg5, Lys28 and the positively charged N-terminus. This further supports the experimental findings that suggest that tight binding[62] to PC-containing bilayers does not affect the secondary structure of Aβ at low peptide concentrations.[64,65] At low concentrations (5 mM) Aβ has been shown to aggregate at the surface of domains rich in POPC, SM and cholesterol.[21,66] Our results revealed how the rigidity of SM compared to that of

POPC reduces the interactions of Aβ42 with the bilayer surface, thus mediating its transition to a β-sheet-enriched structure not observed in the other bilayers, including one that contained 5% GM1. The physiological concentration of GM1 has been shown to be 2-4% of the total lipid content of neurons. Amaro *et al.* have proposed that low concentrations of GM1 facilitates the formation of β-sheets within Aβ42 while at the same time inhibiting its aggregation.[21,67] In our study the β-sheet content at the C-terminus of Aβ42 in the presence of 5%GM1 increased slightly, which may correspond to the increased β-sheet content shown by others, particularly at higher, but less physiologically relevant GM1 concentrations.[19] The disruption of membranes by Aβ has been described by a two-step mechanism, where Aβ oligomers first bind to the membrane to form ion permeable pores, before forming fibrils which concurrently disrupts the membrane via a detergent-like mechanism.[68,69] This study is of the Aβ monomer, so these results do not yet support this hypothesis; however, rigid membranes containing SM could facilitate the conversion of Aβ peptides to a β-sheet-rich state whilst bound to the membrane surface. Subsequent studies on Aβ oligomers could further test this hypothesis.

5 CONCLUSIONS

The increased rigidity of the 30%SM bilayer (30% SM, 40% POPC 30% CHOL) and to a lesser degree 5%GM1 (5% GM1, 70% POPC, 25% CHOL) affected the interactions between Aβ42 and the respective bilayers. The insertion of the N-terminus (Asp1) and the central polar region (Ser26, Asp27 and Lys28) into the bilayers was hampered by the ceramide-containing SM in the 30%SM bilayer and GM1 in the 5%GM1 bilayer, resulting in fewer contacts, hydrogen bonds, and weaker interaction energies between Aβ42 and the respective bilayers. Particularly in 30%SM, the weaker bilayer interactions at the N-terminus of Aβ42 enabled an N-terminal β-sheet to form, with a peak β-sheet propensity observed at Arg5 and Tyr10. Interestingly mouse Aβ neither contains Arg5 nor Tyr10 (due to Arg5Gly and Tyr10Phe substitutions), does not form plaques, nor

Aβ42, sphingomyelin and the GM1 ganglioside do wild-type mice develop Alzheimer's disease.[70,71] Hydrogen bonds with the side chain of Arg5 kept Aβ42 close to the bilayer, thus the N-terminal β-sheet in Aβ42 can be attributed to the increased rigidity of the bilayer due to the inclusion of 30% SM. 5% GM1 alone did not have this effect, thus the neuroprotective role of low concentrations of GM1 is supported by these results.[20,72] The N-terminal residues of Aβ42 are typically disordered, and though these residues can form β-sheets in fibrils,[53] this ceramide-mediated β-structure sheet is the first to be observed in the membrane-associated Aβ monomer. The results of this study shed new light on the role of ceramides in the membrane-mediated Aβ42 β-sheet enrichment responsible for the formation of toxic Aβ42 oligomers. Having identified how sphingomyelin affects the monomeric Aβ42 structure by increasing the rigidity of the bilayer, our plan is to determine this effect on the structure of Aβ42 oligomers.

ACKNOWLEDGEMENTS

M. O. thanks the Helmholtz Postdoc Programmme, and the SoMoPro II programme, co-financed by the European Union and the South-Moravian Region, SoMoPro [Alzheimer's Lipids] - 6SA18009. This publication reflects only the author's views and the Union is not liable for any use that may be made of the information contained herein. W. K., C. P., and T.R. thank the Academy of Finland for financial support (the Finland Distinguished Professor (FiDiPro, Grant no. 263410) program, and the Center of Excellence funding (Grant no. 307415)). The CSC—IT Centre for Science (Espoo, Finland) is acknowledged for excellent computational resources (project number tty3995). We also acknowledge grants of computer capacity from the Finnish Grid and Cloud Infrastructure (persistent identifier urn:nbn:fi:research-infras-201). B. S. and M. O. gratefully acknowledge the computing time granted by the JARA-HPC Vergabegremium on the supercomputer JURECA at Forschungszentrum Jülich (Grant no. JICS68).

REFERENCES

1. Mullane, K.; Williams, M. Biochem. Pharmacol. 2013, 85, 289.
2. Shankar, G. M.; Walsh, D. M. Mol. Neurodegener. 2009, 4, 48-60.
3. Iijima, K.; Liu, H.; Chiang, A.; Hearn, S. A.; Konsolaki, M.; Zhong, Y. Proc. Natl. Acad. Sci. U.S.A. 2004, 101, 6623–6628.
4. Dahlgren, K. N.; Manelli, A. M.; Stine, W. B.; Baker, L. K.; Krafft, G. A.; La Du. M. J. J. Biol. Chem. 2002, 277, 32046–32053.
5. Nagel-Steger, L.; Owen, M. C.; Strodel, B. ChemBioChem 2016, 17, 657-676.
6. Kirkitadze, M. D.; Bitan, G.; Teplow, D. B. J. Neurosci. Res. 2002, 69, 567–577.
7. Philo, J. S.; Arakawa, T. Curr. Pharm. Biotechnol. 2009, 10, 348-351.
8. Yanagisawa, K. Biochem. Biochem. Acta 2007, 1768, 1943-1951.
9. Chiang, H.; Iijima, K.; Hakker, I.; Zhong, Y. FASEB. J. 2009, 23, 1969-1977.
10. Matsuzaki, K.; Kato, K.; Yanagisawa, K. Biochem. Biophys. Acta 2010, 1801, 868-877.
11. Serpell, L. C.; Williams, T. L. FEBS J. 2011, 278, 3905-3917.
12. Yang, X.; Askarova, S.; Lee, J. C. M. Mol. Neurobiol. 2010, 41, 138-148.
13. Devanathan, S.; Salamon, Z.; Lindblom, G.; Groebner, G.; Tollin, G. FEBS J. 2006, 273, 1389-1402.
14. Brown, A. M.; Bevan, D. R. Biophys. J. 2016, 111, 937-949.
15. Di Scala, C.; Chahiniam, H.; Yahl, N.; Garmy, N. Fantini, J. Biochemistry, 2014, 53, 4489-4502.
16. Yu, X.; Yheng, J. J. Mol. Biol. 2011, 421, 561-571.
17. Fernández-Pérez, E. J.; Sepúlveda, F. J.; Peoples, R.; Aguayo, L. G. BBA - Mol. Basis Dis. 2017, 1863, 3105-3116.
18. Nicastro, M.; Spigolon, D.; Librizzi, F.; Moran, O.; Ortone, M. G.; Bulone, D.; San Biagio, P. L.; Carrotta, R. Biophys. Chem. 2016, 208, 9-16.
19. Yanagisawa, K. 2011, 116, 806-812.
20. Ariga, T.; McDonald, M. P.; Yu, R. K. J. Lipid Res. 2008, 49, 1157-1175.
21. Amaro, M.; Šachl, R.; Aydogan, G.; Mikhalyov, I. I.; Vacha, R.; Hof, M. Angew. Chem. Int. Ed. 20156, 55, 9411-9415.
22. Drolle, E.; Negoda, A.; Hammond, K.; Pavlov, E.; Leonenko, Z. PloS ONE. 2017, 12, e0182194.
23. Nasica-Labouze, J.; Nguyen, P. H.; Sterpone, F.; Berthoumieu, O.; et al. Chem. Rev. 2015, 115, 3518-3563.
24. Davis, C. H.; Berkowitz, M. L. Biophys. J. 2009, 96, 785-797.
25. Davis, C. H.; Berkowitz, M. L. J. Phys. Chem. B 2009, 113, 14480-14486.
26. Lemkul, J. A.; Bevan, D. R. FEBS J. 2009, 3060-3075.
27. Lemkul, J. A.; Bevan, D. R. Arch. Biochem. Biophys. 2008, 470, 54-63.
28. Lemkul, J. A.; Bevan, D. R. Biochemistry, 2013, 52, 4971–4980.
29. Strodel, B.; Lee, J. W. L.; Whittleston, C. S.; Wales, D. J. J. Am. Chem. Soc. 2010, 132, 13300-13312.
30. Poojari, C.; Kukol, A.; Strodel, B. Biochim. Biophys. Acta 2013, 1828, 327-339.
31. Poojari, C.; Strodel, B. PloS One 2013, 8, e78399.
32. Lemkul, J. A.; Bevan, D. R Prot. Sci. 2011, 20,1520-1529.
33. Jorgensen, W. L.; Maxwell, D. S.; Tirado-Rives, J. J. Am. Chem. Soc. 1996, 118, 11225-11236.
34. Kaminski, G. A.; Friesner, R. A.; Tirado-Rives, J.; Jorgensen, W. L. J. Phys. Chem. 2001, 105, 6474-6487.
35. Jorgensen, W. L.; Chandrasekhar, J.; Madura, J. D.; Impey, R. W.; Klein, M. L. J. Chem. Phys.

1983, 79, 926-935.
36. Hess, B.; Bekker, H.; Berendsen, H. J. C.; Fraaije, J. G. E. M. J. Comput. Chem. 1997, 18, 1463-1472.
37. Parrinello, M.; Rahman, A. J. Appl. Phys. 1981, 52, 7182-7190.
38. Nosé, S. J. Chem. Phys. 1984, 81, 511-519.
39. Hoover, W. G. Phys. Rev. A 1985, 31, 1695-1697.
40. Essman, U.; Perera, L.; Berkowitz, M. L.; Darden, H. L. T.; Pedersen, L. G. A smooth particle mesh Ewald method. J. Phys. Chem. 1995, 103, 8577-8592.
41. Van der Spoel, D.; Lindahl, E.; Hess, B; and the GROMACS development team. GROMACS User Manual version 4.6.7, www.gromacs.org, 2014.
42. Berendsen, H. J. C.; van der Spoel, D.; van Drunen, R. Comp. Phys. Comm. 1995, 91, 43-56.
43. Hess, B.; Kutzner, C.; van der Spoel, D.; Lindahl, E. J. Chem. Theory Comput. 2008, 4, 435-447.
44. Gapsys, V.; de Groot, B. L.; Briones, R. J. Comput. Aid. Mol. Des. 2013, 27, 845-858.
45. Allen, W.; Lemkul, J.; Bevan, D. J. Comput. Chem. 2009, 30, 12; 1952-1958.
46. Davis, J. H. Biochim. Biophys. Acta 1983, 737, 117-171.
47. Kabsch, W.; Sander, C. Biopolymers 1983, 22, 2577-2637.
48. Daura, X.; Gademann, K.; Juan, B.; Seebach, D. et al. Angew. Chem. 1999, 111, 236-240.
49. Humphrey, W.; Dalke, A.; Schulten, K. et al. J. Molec. Graphics 1996, 14, 33-38.
50. Park, S.; Beaven, A. H.; Klauda, J. B.; Im, W. J. Chem. Theory Comput. 2015, 11, 3466-3477.
51. Ramstedt, B.; Slotte, P. Biochim. Biophys. Acta 2006, 1758, 1945-1956.
52. Ono, K.; Condron, M. M.; Teplow, D. B. Proc. Natl. Acad. Sci. USA 2009, 106, 14745-14750.
53. Rosenman, D. J.; Connors, C. R.; Chen, W.; Wang, C.; Garcia, A. E. J. Mol. Biol. 2013, 425, 3338-3359.
54. Xiao, Y.; Ma, B.; McElheny, D.; Parthasarathy, S. et al. Nat. Struct. Mol. Biol. 2015, 22, 499-505.
55. Colvin, M. T.; Silvers, R.; Ni, Q. Z.; Can, T. V. et al. J. Am. Chem. Soc. 2016, 138, 9663-9674.
56. Waelti, M. A.; Ravotti, F.; Arai, H.; Glabe, C. G. Proc. Natl. Acad. Sci. USA 2016, 113, E4976-E4984.
57. Gremer, L.; Schoelzel, D.; Schenk, C.; Reinartz, E.; et al. Science 2017, 358, 116-119.
58. Ball, K. A.; Phillips, A. H. Nerenberg, P. S. Fawzi, N. L. Wemmer, D. E. Head-Gordon, T. Biochemistry, 2011, 50, 7612-7628.
59. Carballo-Pacheco, M.; Strodel, B. Protein Sci. 2016, 26, 174-185.
60. Yan, Y.; Wang, C. J. Mol. Biol. 2006, 364, 853-862.
61. Wu, C.; Murray, M. M.; Bernstein, S. L.; Condron, M. M.; Bitan, G. Shea, J. E.; Bowers, M. T. J. Mol. Biol. 387, 492-501.
62. Ding, H.; Schauerte, J. A.; Steel. D. G.; Gafni, A. Biophys. J. 2012, 103, 1500-1509.
63. Korshavn, K.; Satriano, C.; Lin, Y.; Yhang, R.; Dulchavsky, M.; et al. J. Biol. Chem. 2017, 292, 4638-4650.
64. Qiang, W.; Yau, W.; Schulte, J. Biochim. Biophys. Acta 2015, 1848, 266-276.
65. Terzi, E.; Hoezlmann, G.; Seeling, J. J. Mol. Biol. 1995, 252, 633-642.
66. Devanathan, S.; Salamon, Z.; Lindblom, G.; Groebner, G.; Tollin, G. FEBS J. 1389-1402.
67. Cebecauer, M.; Hof, M.; Amaro, M. Biophys. J. 2017, 113, 1197-1199.
68. Sciacca, M. F. M.; Milardi, D.; Messina, G. M. L.; Marletta, G.; Brender, J. R.; Ramamoorthy, A.; La Rosa, C. Biophys. J. 2013, 104, 173-184.
69. Kotler, S. A.; Walsh, P. W.; Brender, J. R., Ramamoorthy, A. Chem Soc. Rev. 2014, 43, 6692-6700.
70. Kitazawa, M.; Medeiros, R.; LaFerla, F. M. Curr. Pharm. Des. 2012, 18, 1131-1147.

71. Dyrks, T.; Dyrks, E.; Masters, C. L.; Beyreuther, K. FEBS J. 1993, 324, 231-236.
72. Mocchetti, I. Cell. Mol. Life Sci. 2005, 62, 2283-2294.

Highlights

To our knowledge, this is the first molecular dynamics (MD) simulation study which systematically studies the effects of physiologically relevant membrane compositions on the structure of Aβ42.
In particular, following bilayers were considered: 70% POPC + 30% cholesterol; 30% SM+ 40% POPC + 30% cholesterol; 5% GM1+ 70% POPC + 25% cholesterol.
The formation of a β-sheet in the normally disordered N-terminal region of Aβ42 was observed as a result of the increased bilayer rigidity provided by SM.
With β-sheets at the N and C termini, the structure of Aβ42 in the sphingomyelin-enriched bilayer most resembles β-sheet-rich structures found in higher-ordered Aβ fibrils.
Conversely, when bound to a bilayer comprised of 5% GM1, the conformation remained similar to that observed in the absence of GM1, with Aβ42 only making contact with one or two GM1 molecules.